Available online at www.sciencedirect.com
ScienceDirect
Inorganica Chimica Acta 360 (2007) 1651–1660
Inorganica Chimica Acta
www.elsevier.com/locate/ica

Synthesis of $[SnPh_2(SR^F)_2]$ $SR^F = {}^-SC_6F_4$-4-H, ${}^-SC_6F_5$: Reactivity towards group 10 transition metal complexes

Fabiola Estudiante-Negrete [a], Rocío Redón [b], Simón Hernández-Ortega [a], Rubén A. Toscano [a], David Morales-Morales [a,*]

[a] *Instituto de Química, Universidad Nacional Autónoma de México, Cd. Universitaria, Circuito Exterior, Coyoacán, 04510 México D.F., Mexico*
[b] *Centro de Ciencias Aplicadas y Desarrollo Tecnológico (CCADET), UNAM. Cd. Universitaria, Circuito Exterior, Coyoacán, 04510 México D.F., Mexico*

Received 21 July 2006; received in revised form 31 August 2006; accepted 1 September 2006
Available online 20 September 2006

Abstract

The organometallic tin(IV) complexes $[SnPh_2(SR^F)_2]$ $SR^F = {}^-SC_6F_4$-4-H (**1**), ${}^-SC_6F_5$ (**2**), were synthesized and their reactivity with $[MCl_2(PPh_3)_2]$ M = Ni, Pd and Pt explored. Thus, transmetallation products were obtained affording polymeric $[Ni(SR^F)(\mu\text{-}SR^F)]_n$, monomeric *cis*-$[Pt(PPh_3)_2(SC_6F_4\text{-}4\text{-}H)_2]$ (**3**) and *cis*-$[Pt(PPh_3)_2(SC_6F_5)_2]$ (**4**) and dimeric species $[Pd(PPh_3)(SC_6F_4\text{-}4\text{-}H)(\mu\text{-}SC_6F_4\text{-}4\text{-}H)]_2$ (**5**) and $[Pd(PPh_3)(SC_6F_5)(\mu\text{-}SC_6F_5)]_2$ (**6**) for Ni, Pt and Pd, respectively. The crystal structures of complexes **1**, **2**, **3**, **4** and **6** were determined.

Keywords: Thiolate ligands; Transmetallation; Transition metal complexes; Tin complexes; Crystal structures

1. Introduction

Tin complexes have acquired a raising interest in recent years due to the applications that these compounds have found in fields such as medicinal and bioinorganic chemistry [1], having an important impact in the design of new species for therapeutic use in the treatment of different illnesses, including different types of cancer [2]. Tin complexes have also been successfully employed in other areas of chemistry such as self assembly, molecular recognition and catalysis [3]. In this respect, processes involving transmetallation reactions as key steps for a particular catalytic reaction have been of considerable interest in recent years. Being this particularly true for reactions involving the formation of C–C bonds and of particular interest the Stille reaction [4] which uses organometallic tin complexes as starting materials and where the transmetallation process is the rate-determining step [5].

Moreover, thiolate complexes have been used profusely due the relevance that these ligands have had in the design of complexes able to mimic the biological functions of active centers of different metalloenzymes like nitrogenase [6]. Additionally, given the facility with which thiols can be tuned both steric and electronically, they have been widely used as auxiliary ligands [7]. Hence, the presence of electron-withdrawing groups or substituents with steric requirements favor the formation of mononuclear complexes rather than the thiolate bridged oligomers, usually generated by using unencumbered thiols [8]. Moreover, thiolate complexes are known to undergo chemistry at the sulfur center, including redox and protonation–deprotonation processes a plus to traditional chemistry for these complexes usually centered on the metal [9]. Thus, following our current interest in the synthesis, structural studies and reactivity of thiolate metal complexes [10], we would like to report here the synthesis of organometallic tin(IV)

* Corresponding author. Tel.: +52 55 56224514; fax: +52 55 56162217.
E-mail address: damor@servidor.unam.mx (D. Morales-Morales).

0020-1693/$ - see front matter © 2006 Elsevier B.V. All rights reserved.
doi:10.1016/j.ica.2006.09.003

complexes with the thiols HSC_6F_5 and HSC_6F_4-4-H and their reactivity towards group 10 transition metal complexes.

2. Experimental

2.1. Materials and methods

Unless stated otherwise, all reactions were carried out under an atmosphere of dinitrogen using conventional Schlenk glassware, solvents were dried using established procedures and distilled under dinitrogen immediately prior to use. The IR spectra were recorded on a Nicolet-Magna 750 FT-IR spectrometer as nujol mulls. The ^1H NMR spectra were recorded on a JEOL GX300 spectrometer. Chemical shifts are reported in ppm down field of TMS using the solvent ($CDCl_3$, $\delta = 7.27$) as internal standard. $^{31}P\{^1H\}$, $^{19}F\{^1H\}$ and $^{119}Sn\{^1H\}$ spectra were recorded with complete proton decoupling and are reported in ppm using 85% H_3PO_4, C_6F_6 or $SnMe_4$ as external standards, respectively. Elemental analyses were determined on a Perkin–Elmer 240. Positive-ion FAB mass spectra were recorded on a JEOL JMS-SX102A mass spectrometer operated at an accelerating voltage of 10 kV. Samples were desorbed from a nitrobenzyl alcohol (NOBA) matrix using 3 keV xenon atoms. Mass measurements in FAB are performed at a resolution of 3000 using magnetic field scans and the matrix ions as the reference material or, alternatively, by electric field scans with the sample peak bracketed by two (polyethylene glycol or cesium iodide) reference ions. Melting points were determined in a MEL-TEMP capillary melting point apparatus and are reported without correction.

The complex $[SnPh_2(Cl)_2]$ and the $PdCl_2$, $PtCl_2$, $NiCl_2$ metal salts and thiols HSC_6F_4-4-H and HSC_6F_5 were obtained commercially from Aldrich Chem. Co. Compounds *trans*-$[NiCl_2(PPh_3)_2]$ [11], *trans*-$[PdCl_2(PPh_3)_2]$ [12], *cis*-$[PtCl_2(PPh_3)_2]$ [13], and $[Pb(SR^F)_2]$, $SR^F = {}^-SC_6F_5$, ${}^-SC_6F_4$-4-H [14]. were synthesized according to the published procedures.

2.2. Synthesis of $[SnPh_2(SC_6F_4\text{-}4\text{-}H)_2]$ (1)

To a CH_2Cl_2 solution (30 mL) of $[SnPh_2(Cl)_2]$ (100 mg, 0.29 mmol) a suspension of $[Pb(SC_6F_4\text{-}4\text{-}H)_2]$ (165 mg, 0.29 mmol) in CH_2Cl_2 (50 mL) was slowly added. The resulting solution was allowed to proceed under stirring for 12 h. After this time the resulting solution was filtered trough a short plug of celite and the residue washed twice with CH_2Cl_2 (30 mL) to afford 164 mg of a microcrystalline white powder. Yield: 89%. M.p. 73–75 °C. RMN-^1H (300 MHz, $CDCl_3$), δ 7.49–7.40 (m, Ph, 10H), 6.80–6.74 (m, SC_6F_4-4-H, 2H); RMN-$^{19}F\{^1H\}$ (282 MHz, $CDCl_3$), δ −129.37 (m, *o*-F), −137.76 (m, *m*-F); RMN-$^{119}Sn\{^1H\}$ (112 MHz, $CDCl_3$), δ 13.81 ppm (s). Elemental *Anal*. Calc. for $[C_{24}H_{12}F_8S_2Sn]$: C, 45.38; H, 1.90. Found: C, 45.25; H, 1.83%. MS-FAB$^+$ $[M^+] = 635$ *m*/*z*.

2.3. Synthesis of $[SnPh_2(SC_6F_5)_2]$ (2)

To a CH_2Cl_2 solution (30 mL) of $[SnPh_2(Cl)_2]$ (100 mg, 0.29 mmol) a solution of $[Pb(SC_6F_5)_2]$ (176 mg, 0.29 mmol) in CH_2Cl_2 (50 mL) was slowly added. The resulting solution was allowed to proceed under stirring for 12 h. After this time the resulting solution was filtered trough a short plug of celite and the residue washed twice with CH_2Cl_2 (30 mL) to afford 166 mg of a microcrystalline white powder. Yield: 85%. M.p. 58–60 °C. RMN-^1H (300 MHz, $CDCl_3$), δ 7.47–7.43 (m, Ph, 10H); RMN-$^{19}F\{^1H\}$ (282 MHz, $CDCl_3$), δ −129.88 (dd, $^3J_{F_o-F_m} = 24.00$ Hz, $^4J_{F_o-F_p} = 7.05$ Hz, *o*-F), −155.14 (bt, $^3J_{F_p-F_m} = 21.20$ Hz, *p*-F), −161.87 (m, $^3J_{F_o-F_m} = 23.26$ Hz, $^4J_{F_m-F_p} = 7.05$ Hz, *m*-F); RMN-$^{119}Sn\{^1H\}$ (112 MHz, $CDCl_3$), δ 18.09 ppm (s). Elem. *Anal*. Calc. for $[C_{24}H_{10}F_{10}S_2Sn]$: C, 42.95; H, 1.50. Found: C, 42.58; H, 1.42%. MS-FAB$^+$ $[M^+-Ph] = 595$ *m*/*z*.

2.4. Synthesis of cis-$[Pt(PPh_3)_2(SC_6F_4\text{-}4\text{-}H)_2]$ (3)

To a solution of $[Sn(Ph)_2(SC_6F_4\text{-}4\text{-}H)_2]$ (100 mg, 0.156 mmol) in CH_2Cl_2 (20 mL), a solution of *cis*-$[Pt(PPh_3)_2(Cl)_2]$ (123 mg, 0.156 mmol) in CH_2Cl_2 (20 mL) was added dropwise under stirring, the resulting yellow-green solution was allowed to stir overnight, after which time the pale green precipitate formed was filtered out and recrystallized from CH_2Cl_2–hexane, to afford **3** as a yellow-green microcrystalline powder. 147 mg, Yield: 87%. M.p. 183–185 °C. NMR ^1H (300 MHz, $CDCl_3$), δ 7.7–7.1 (m, Ph, 32H); NMR $^{31}P\{^1H\}$ (121 MHz, $CDCl_3$), δ 19.12 (s, $^1J_{P-Pt} = 3.1$ kHz, P); NMR $^{19}F\{^1H\}$ (282 MHz, $CDCl_3$), δ −133.85 (bm, $^3J_{F_o-F_m} = 23.97$Hz, $^5J_{F_o-F_m} = 8.04$ Hz, *o*-F), −142.11 (m, $^3J_{F_o-F_m} = 25.10$ Hz, $^5J_{F_o-F_m} = 10.43$ Hz, $^4J_{F_o-F_m} = 10.15$ Hz, *m*-F). Elem. *Anal*. Calc. for $[C_{48}H_{32}F_8P_2PtS_2]$: C, 53.29; H; 2.98. Found: C, 53.24; H, 2.86%. MS-FAB$^+$ $[M^+] = 1081$ *m*/*z*.

2.5. Synthesis of cis-$[Pt(PPh_3)_2(SC_6F_5)_2]$ (4)

To a solution of $[Sn(Ph)_2(SC_6F_5)_2]$ (100 mg, 0.149 mmol) in CH_2Cl_2 (20 mL), a solution of *cis*-$[Pt(PPh_3)_2(Cl)_2]$ (117 mg, 0.149 mmol) in CH_2Cl_2 (20 mL) was added dropwise under stirring, the resulting yellow-green solution was allowed to stir overnight, after which time the green precipitate formed was filtered out and recrystallized from CH_2Cl_2–hexane, to afford **4** as a green-yellow microcrystalline powder. 142 mg, Yield: 85%. M.p. 170–172 °C. NMR ^1H (300 MHz, $CDCl_3$), δ 7.7–7.1 (m, Ph, 30H); NMR $^{31}P\{^1H\}$ (121 MHz, $CDCl_3$), δ 18.85 (s, $^1J_{P-Pt} = 3.1$ kHz, P); NMR $^{19}F\{^1H\}$ (282 MHz, $CDCl_3$), δ −133.65 (dd, $^3J_{F_o-F_m} = 26.22$ Hz, $^4J_{F_o-F_p} = 6.20$ Hz, *o*-F), −161.98 (bt, $^4J_{F_o-F_p} = 23.69$ Hz, *p*-F), −164.88 (m, $^3J_{F_o-F_m} = 23.62$ Hz, $^4J_{F_o-F_p} = 7.19$ Hz, *m*-F). Elem. *Anal*. Calc. for $[C_{48}H_{30}F_{10}P_2PtS_2]$: C, 51.57; H, 2.70. Found: C, 51.48; H, 2.68%. MS-FAB$^+$ $[M^+] = 1117$ *m*/*z*.

2.6. Synthesis of [Pd(PPh$_3$)(SC$_6$F$_4$-4-H)(μ-SC$_6$F$_4$-4-H)]$_2$ (5)

To a solution of [Sn(Ph)$_2$(SC$_6$F$_4$-4-H)$_2$] (100 mg, 0.156 mmol) in CH_2Cl_2 (20 mL), a solution of *trans*-[Pd(PPh$_3$)$_2$(Cl)$_2$] (109 mg, 0.156 mmol) in CH_2Cl_2 (20 mL) was added dropwise under stirring, the resulting yellow-orange solution was allowed to stir overnight, after this time the solution was filtered and the solvent removed under vacuum. The residue was recrystallized from CH_2Cl_2–hexane, to afford **5** as an orange microcrystalline powder. 196 mg, Yield: 85%. M.p. 182–183 °C. Elem. *Anal.* Calc. for [C$_{60}$H$_{34}$F$_{16}$P$_2$Pd$_2$S$_4$]: C, 49.29; H, 2.34. Found: C, 49.15; H, 2.28%. MS-FAB$^+$ [M$^+$−SC$_6$F$_4$-4-H] = 1381 *m*/*z*.

2.7. Synthesis of [Pd(PPh$_3$)(SC$_6$F$_5$)(μ-SC$_6$F$_5$)]$_2$ (6)

To a solution of [Sn(Ph)$_2$(SC$_6$F$_5$)$_2$] (100 mg, 0.149 mmol) in CH_2Cl_2 (20 mL), a solution of *trans*-[Pd(PPh$_3$)$_2$(Cl)$_2$] (104 mg, 0.149 mmol) in CH_2Cl_2 (20 mL) was added dropwise under stirring, the resulting red-orange solution was allowed to stir overnight, after this time the solution was filtered and the solvent removed under vacuum. The residue was recrystallized from CH_2Cl_2–hexane, to afford **6** as a red microcrystalline powder. 203 mg, Yield: 89%. M.p. 264–265 °C. NMR ^{1}H (300 MHz, $CDCl_3$, 330 K), δ 7.7–7.1 (m, Ph, 30H); NMR ^{31}P{^{1}H} (121 MHz, $CDCl_3$, 330 K), δ 28.2 (s, P); NMR ^{19}F{^{1}H} (282 MHz, $CDCl_3$, 330 K), δ −126.2 (bm, *o*-F bridge), −131.3 (m, *o*-F terminal), −148.0 (m, *p*-F bridge), −155.5 (m, *p*-F terminal), −159.6 (m, *m*-F bridge), −163.5 (m, *m*-F terminal). Elem. *Anal.* Calc. for [C$_{60}$H$_{30}$F$_{20}$P$_2$Pd$_2$S$_4$]: C, 46.98; H, 1.97. Found: C, 46.51; H, 2.01%. MS-FAB$^+$ [M$^+$−SC$_6$F$_5$] = 1335 *m*/*z*.

2.8. Data collection and refinement for [SnPh$_2$(SC$_6$F$_4$-4-H)$_2$] (1), [SnPh$_2$(SC$_6$F$_5$)$_2$](2), cis-[Pt(PPh$_3$)$_2$(SC$_6$F$_4$-4-H)$_2$] (3), cis-[Pt(PPh$_3$)$_2$(SC$_6$F$_5$)$_2$] (4), [Pd(PPh$_3$)(SC$_6$F$_5$)(μ-SC$_6$F$_5$)]$_2$ (6)

Crystalline colorless prisms of **1** and **2**, yellow prisms of **3** and **4** and a reddish prism of **5** grown independently from CH_2Cl_2/MeOH solvent systems were glued each to glass fibers. The X-ray intensity data were measured at 291 K for **1**, **2** and **3** and at 293 K for **4** and **6** on a Bruker

Table 1
Summary of crystal structure data for [SnPh$_2$(SC$_6$F$_4$-4-H)$_2$] (**1**), [SnPh$_2$(SC$_6$F$_5$)$_2$] (**2**) *cis*-[Pt(PPh$_3$)$_2$(SC$_6$F$_4$-4-H)$_2$] (**3**), *cis*-[Pt(PPh$_3$)$_2$(SC$_6$F$_5$)$_2$] (**4**), [Pd(PPh$_3$)(SC$_6$F$_5$)(μ-SC$_6$F$_5$)]$_2$ (**6**)

Compound	[SnPh$_2$(SC$_6$F$_4$-4-H)$_2$] (**1**)	[SnPh$_2$(SC$_6$F$_5$)$_2$] (**2**)	*cis*-[Pt(PPh$_3$)$_2$-(SC$_6$F$_4$-4-H)$_2$] (**3**)	*cis*-[Pt(PPh$_3$)$_2$-(SC$_6$F$_5$)$_2$] (**4**)	[Pd(PPh$_3$)(SC$_6$F$_5$)(μ-SC$_6$F$_5$)]$_2$ (**6**)
Empirical formula	C$_{24}$H$_{12}$F$_8$S$_2$Sn	C$_{24}$H$_{10}$F$_{10}$S$_2$Sn	C$_{49}$H$_{32}$Cl$_2$F$_8$P$_2$PtS$_2$	C$_{49}$H$_{32}$F$_{10}$OP$_2$PtS$_2$	C$_{61}$H$_{31}$C$_{13}$F$_{20}$P$_2$Pd$_2$S$_4$
Formula weight	635.15	671.13	1164.80	1135.89	1653.19
Temperature (K)	291(2)	291(2)	291(2)	293(2)	293(2)
Crystal system	monoclinic	triclinic	monoclinic	monoclinic	monoclinic
Space group	$P2_1/c$	$P\bar{1}$	$P2_1/n$	$C2/c$	$P2_1/c$
Crystal size (mm)	0.26 × 0.22 × 0.04	0.32 × 0.26 × 0.22	0.30 × 0.14 × 0.12	0.406 × 0.128 × 0.036	0.178 × 0.178 × 0.158
Unit cell dimensions					
a (Å)	11.9083(7)	9.5051(6)	14.8746(8)	31.816(2)	10.0622(5)
b (Å)	7.3992(4)	10.6793(6)	19.602(1)	13.9880(8)	17.5843(9)
c (Å)	27.345(2)	12.6904(7)	17.5800(9)	20.419(1)	19.270(1)
α (°)	90	82.128(1)	90	90	90
β (°)	90.011(1)	73.950(1)	94.691(1)	90.626(1)	99.209(1)
γ (°)	90	74.022(1)	90°	90	90
Volume (Å^3)	2409.4(2)	1187.55(12)	5108.8(5)	9086.8(9)	3365.6(3)
Z	4	2	4	8	2
Density (g/cm^3)	1.751	1.877	1.514	1.661	1.631
θ Range for data collection (°)	1.71–25.00	2.30–25.00	1.56–25.00	1.28–25.05	1.58–25.00
Reflections collected	18 990	9810	41 500	36 763	27 257
Independent reflections [R_{int}]	4247 [0.0470]	4184 [0.0272]	9003 [0.0492]	8041 [0.0711]	5913 [0.0738]
F(000)	1240	652	2288	4464	1628
Absorption correction	analytical	analytical	analytical	analytical	analytical
Goodness-of-fit on F^2	0.986	1.006	0.883	0.985	0.992
R indices (all data)	$R_1 = 0.0726$, $wR_2 = 0.0978$	$R_1 = 0.0294$, $wR_2 = 0.0638$	$R_1 = 0.0438$, $wR_2 = 0.0667$	$R_1 = 0.0703$, $wR_2 = 0.1120$	$R_1 = 0.1009$, $wR_2 = 0.2429$
Final *R* indices [$I > 2\sigma(I)$]	$R_1 = 0.0479$, $wR_2 = 0.0919$	$R_1 = 0.0263$, $wR_2 = 0.0627$	$R_1 = 0.0302$, $wR_2 = 0.0645$	$R_1 = 0.0432$, $wR_2 = 0.0981$	$R_1 = 0.0767$, $wR_2 = 0.2224$
Data/restrains/parameters	4247/0/316	4184/0/334	9003/0/570	8041/0/584	5913/0/417
Index ranges	$-14 \leqslant k \leqslant 14$, $-8 \leqslant h \leqslant 8$, $-32 \leqslant l \leqslant 32$	$-11 \leqslant k \leqslant 11$, $-12 \leqslant h \leqslant 12$, $-15 \leqslant l \leqslant 15$	$-17 \leqslant k \leqslant 17$, $-23 \leqslant h \leqslant 23$, $-20 \leqslant l \leqslant 20$	$-37 \leqslant k \leqslant 37$, $-16 \leqslant h \leqslant 16$, $-24 \leqslant l \leqslant 24$	$-11 \leqslant k \leqslant 11$, $-20 \leqslant h \leqslant 20$, $-22 \leqslant l \leqslant 22$

SMART APEX CCD-based X-ray diffractometer system equipped with a Mo-target X-ray tube ($\lambda = 0.71073$ Å). The detector was placed at a distance of 4.837 cm. from the crystals in all cases. A total of 1800 frames were collected with a scan width of 0.3 ° in ω and an exposure time of 10 s/frame. The frames were integrated with the Bruker SAINT software package using a narrow-frame integration algorithm. The integration of the data was done using a monoclinic unit cell for **1**, **3**, **4** and **6** or a triclinic unit cell for **2** to yield a total of 18 990 (**1**) 9810 (**2**) 41 500 (**3**) 36 763 (**4**) and 27 257 (**6**) reflections, respectively to a maximum 2θ angle of 50.00° (0.93 Å resolution), of which 4247 (**1**) 4184 (**2**) 9003 (**3**) 8041 (**4**) and 5913 (**6**) were independent. Analysis of the data showed in the three cases negligible decays during data collection. The structures were solved by Patterson method using SHELXS-97 [15] program. The remaining atoms were located via a few cycles of least squares refinements and difference Fourier maps, using the space groups $P2_1/c$ with $Z = 4$ (**1**), $P\bar{1}$ with $Z = 2$ (**2**), $P2_1/n$ with $Z = 4$ (**3**), $C2/c$ with $Z = 8$ (**4**) and $P2_1/c$ with $Z = 2$ (**6**), respectively. Hydrogen atoms were input at calculated positions, and allowed to ride on the atoms to which they are attached. Thermal parameters were refined for hydrogen atoms on the phenyl groups using a $U_{eq} = 1.2$ Å to precedent atom. The final cycle of refinement was carried out using SHELXL-97 [16] and anisotropic thermal parameters for all non-hydrogen atoms. The details of the structure determinations are given in Table 1 and selected bond lengths (Å) and angles (°) and the numbering of the atoms is shown in Figs. 1 and 3–6, respectively (ORTEP) [17].

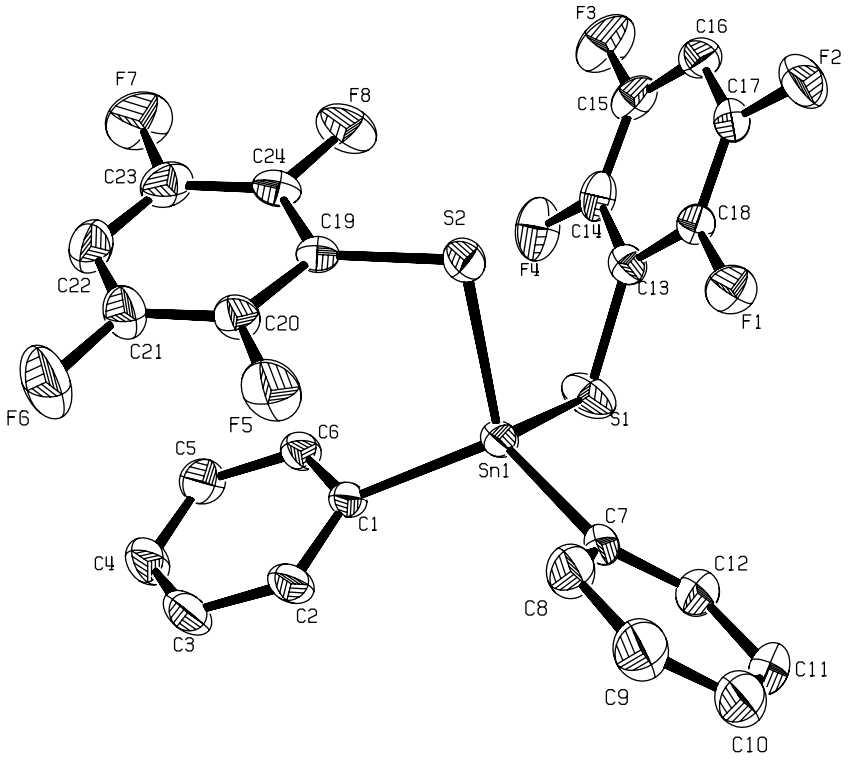

Fig. 1. An ORTEP representation of the structure of $[SnPh_2(SC_6F_4\text{-}4\text{-}H)_2]$ (**1**) at 50% of probability showing the atom labeling scheme. Bond lengths (Å): Sn(1)–C(1) 2.104(5), Sn(1)–C(7) 2.110(6), Sn(1)–S(1) 2.4223(17), Sn(1)–S(2) 2.4231(15). Bond angles (°): C(1)–Sn(1)–C(7) 117.79(19), C(1)–Sn(1)–S(1) 104.56(15), C(7)–Sn(1)–S(1) 111.43(19), C(1)–Sn(1)–S(2) 107.10(14), C(7)–Sn(1)–S(2) 108.86(17), S(1)–Sn(1)–S(2) 106.44(6).

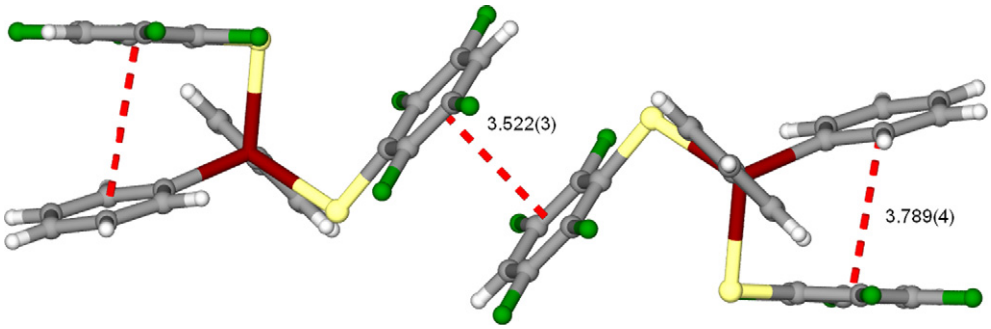

Fig. 2. X-SEED [28] representation of the intramolecular and intermolecular π–π stacking interactions observed in complex $[SnPh_2(SC_6F_4\text{-}4\text{-}H)_2]$ (**1**).

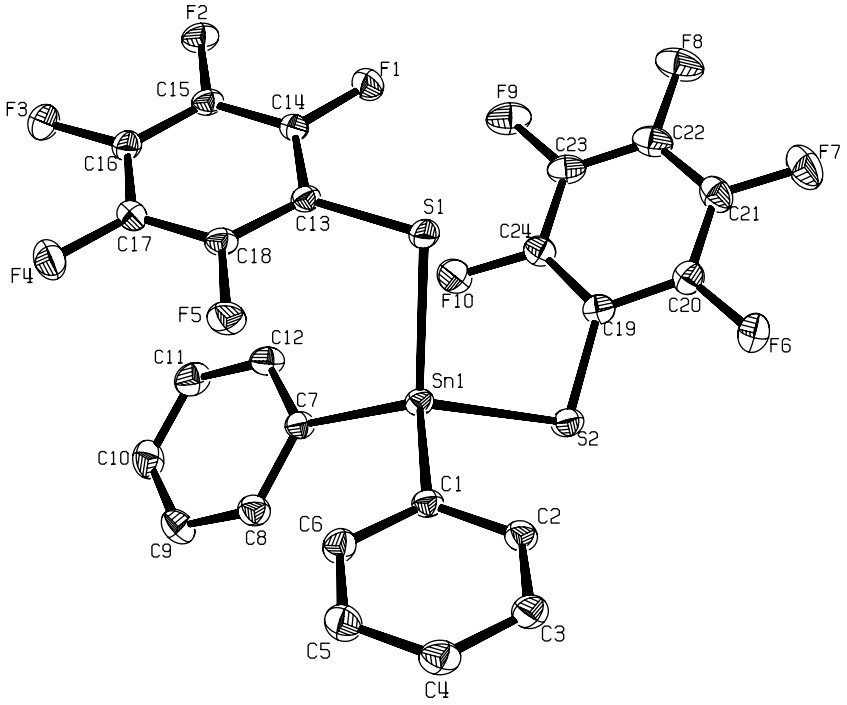

Fig. 3. An ORTEP representation of the structure of $[SnPh_2(SC_6F_5)_2]$ (**2**) at 50% of probability showing the atom labeling scheme. Bond lengths (Å): Sn(1)–C(7) 2.128(2), Sn(1)–C(1) 2.130(2), Sn(1)–S(2) 2.4329(8), Sn(1)–S(1) 2.4331(7). Bond angles (°): C(7)–Sn(1)–C(1) 112.63(10), C(7)–Sn(1)–S(2) 114.66(7), C(1)–Sn(1)–S(2) 104.11(7), C(7)–Sn(1)–S(1) 110.85(7), C(1)–Sn(1)–S(1) 109.92(7), S(2)–Sn(1)–S(1) 104.14(3).

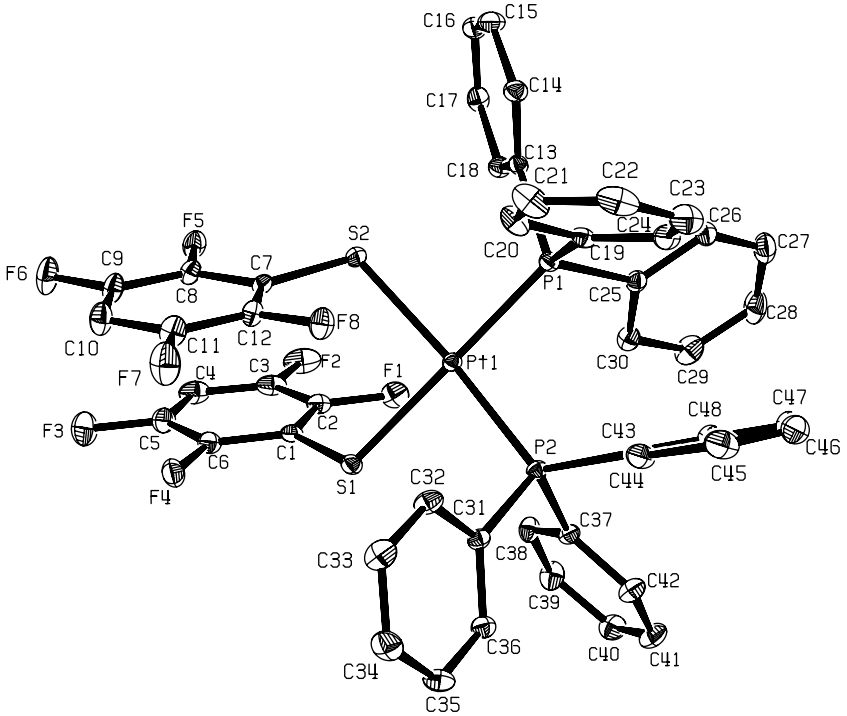

Fig. 4. An ORTEP representation of the structure of *cis*-$[Pt(PPh_3)_2(SC_6F_4\text{-}4\text{-}H)]$ (**3**) at 50% of probability showing the atom labeling scheme. Bond lengths (Å): Pt(1)–P(1) 2.2806(11), Pt(1)–P(2) 2.2969(11), Pt(1)–S(2) 2.3621(11), Pt(1)–S(1) 2.3733(11). Bond angles (°): P(1)–Pt(1)–P(2) 96.54(4), P(1)–Pt(1)–S(2) 87.05(4), P(2)–Pt(1)–S(2) 171.07(4), P(1)–Pt(1)–S(1) 177.04(4), P(2)–Pt(1)–S(1) 84.65(4), S(2)–Pt(1)–S(1) 92.17(4)

3. Results and discussion

The reaction in an 1:1 molar ratio of $[SnPh_2(Cl)_2]$ and $[Pb(SC_6F_4\text{-}4\text{-}H)_2]$ or $[Pb(SC_6F_5)_2]$ resulted on the formation of complexes $[SnPh_2(SC_6F_4\text{-}4\text{-}H)_2]$ (**1**) and $[SnPh_2(SC_6F_5)_2]$ (**2**) in good yields (Scheme 1). Analysis of both complexes by ^1H NMR reveals the presence of the phenyl substituents with signals in the typical region

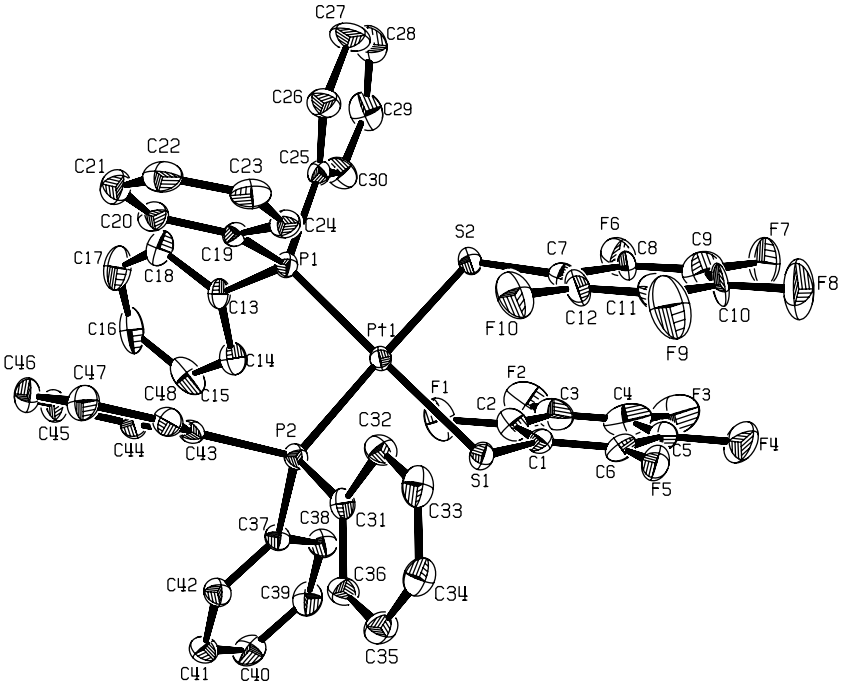

Fig. 5. An ORTEP representation of the structure of *cis*-[Pt(PPh_3)$_2$(SC_6F_5)] (**4**) at 50% of probability showing the atom labeling scheme. Bond lengths (Å): Pt(1)–P(1) 2.282(2), Pt(1)–P(2) 2.297(2), Pt(1)–S(2) 2.344(2), Pt(1)–S(1) 2.372(2). Bond angles (°): P(1)–Pt(1)–P(2) 96.31(7), P(1)–Pt(1)–S(2) 85.90(8), P(2)–Pt(1)–S(2) 174.21(8), P(1)–Pt(1)–S(1) 177.03(7), P(2)–Pt(1)–S(1) 85.38(7), S(2)–Pt(1)–S(1) 92.65(8).

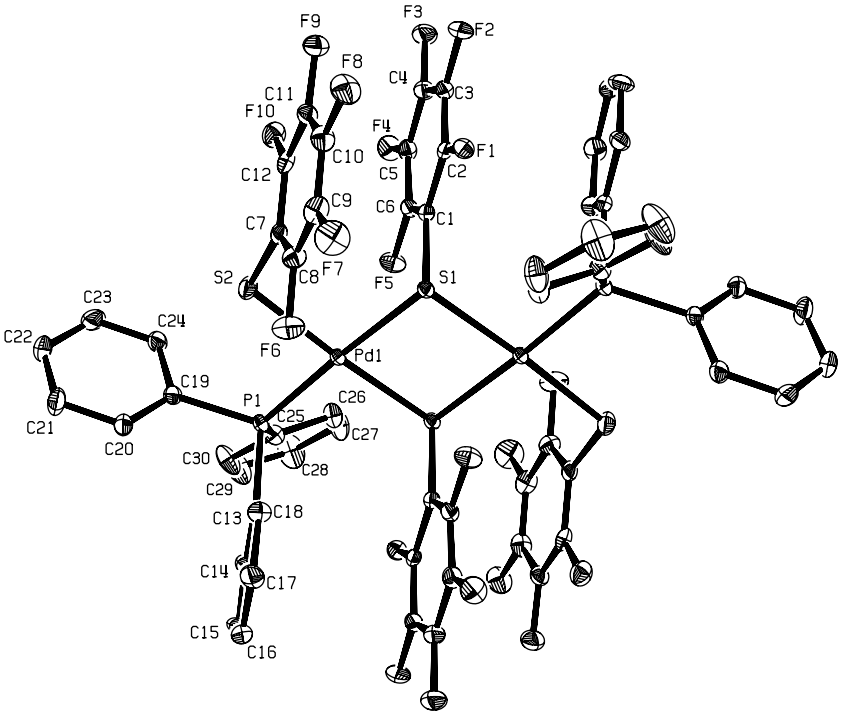

Fig. 6. An ORTEP representation of the structure of [Pd(PPh_3)(SC_6F_5)(μ-SC_6F_5)]$_2$ (**6**) at 50% of probability showing the atom labeling scheme. Bond lengths (Å): Pd(1)–P(1) 2.286(2), Pd(1)–S(2) 2.306(2), Pd(1)–S(1)#1 2.365(2), Pd(1)–S(1) 2.381(2), S(1)–Pd(1)#1 2.365(2). Bond angles (°): P(1)–Pd(1)–S(2) 87.90(8), P(1)–Pd(1)–S(1)#1 95.28(7), S(2)–Pd(1)–S(1)#1 176.67(8), P(1)–Pd(1)–S(1) 176.90(8), S(2)–Pd(1)–S(1) 95.20(8), S(1)#1–Pd(1)–S(1) 81.63(7), Pd(1)#1–S(1)–Pd(1) 98.37(7).

for aromatic protons, additionally the ^{1}H NMR spectrum of complex **1** exhibits a multiplet centered at 6.77 ppm due to the aromatic protons in the *para* position of the thiolates in $^{-}SC_6F_4$-4-**H**, the fact that we are observing only a single signal for these protons clearly indicates magnetic equivalence of the two $^{-}SC_6F_4$-4-**H** substituents. Further

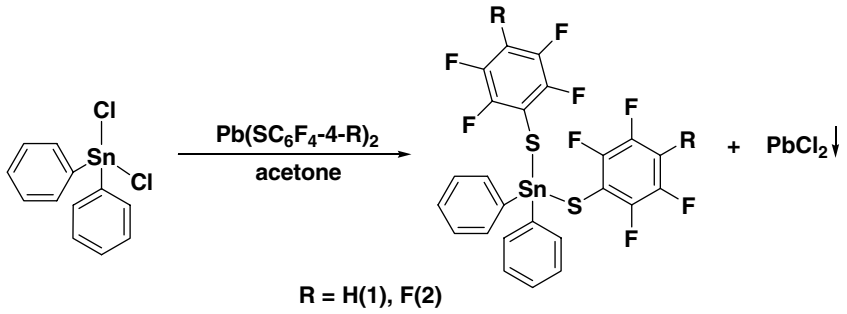

Scheme 1. Synthesis of the $[SnPh_2(SR^F)_2]$ $SR^F = {}^-SC_6F_4$-4-H (**1**) and $^-SC_6F_5$ (**2**) complexes.

analysis of complex **1** by $^{19}F\{^1H\}$ shows signals due to the fluorinated ligands $^-SC_6\mathbf{F}_4$-4-H with multiplets at −129.37 and −137.76 ppm due to the fluorines in the *ortho* and *meta* positions, respectively. A similar behavior is observed for complex **2** where signals due to the *ortho*, *para* and *meta* fluorines in $^-SC_6\mathbf{F}_5$ are observed at −129.88, −155.14 and −161.87 ppm, respectively. Interestingly, analysis by $^{119}Sn\{^1H\}$ NMR reveal the electron-withdrawing effect of the fluorinated substituents over the tin center, thus single signals due to the unique tin centers in complexes **1** and **2** are observed at 13.81 and 18.09 ppm, respectively exhibiting the more pronounced electron-withdrawing effect of the ligand $^-SC_6F_5$. Analysis by FAB^+-MS shows peaks at 635 and 595 *m*/*z* due the molecular ion of complex **1** and the molecular ion less a phenyl group for **2**, respectively. Elemental analyses on both cases are in agreement with the proposed formulations.

Crystals suitable for single crystal X-diffraction analysis were obtained for both complexes. Given the structural similitude of these complexes they share also a number of common features, thus both tin centers are located into slightly distorted tetrahedral environments. The Sn–S distances Sn(1)–S(1) 2.4223 (17) and Sn(2)–S(2) 2.4231 (15) in complex **1** (Fig. 1) are slightly shorter than those found in complex **2** (Fig. 3). A closer analysis of the crystal structure of complex $[SnPh_2(SC_6F_4\text{-}4\text{-}H)_2]$ (**1**) reveals two π–π stacking interactions in the crystal [18], one intermolecular between the $^-SC_6F_4H$ and one $-C_6H_5$ ring and the other intramolecular between the $^-SC_6F_4H$ rings of two molecules (Fig. 2). The π–π intermolecular interactions is given between the C1–C6 and C19–C24 aromatic rings, the angle between the rings is 18°, and the centroid–centroid distance is 3.789(4) Å, the perpendicular distance between the rings is between 3.49 and 3.57 Å. The C13–C18 ring interacts with the C13–C18 ring of a molecule at, $1-x$, $1-y$, $-z$; the rings are parallel with centroid–centroid distance of 3.522(3) Å and a perpendicular distance of 3.49 Å. This stacking interactions seem to reduce the angle S(2)–Sn–C(1) (107.10(4) versus 110.85(7) in **2**), it is also probable that as result of these stacking interactions observed for complex **1**, the bond distances would also be affected thus having as ultimate consequence their shortening (Fig. 2).

With these complexes in hand, reactions using group 10 transition metal starting materials were attempted. Thus, stoichiometric reactions of $[SnPh_2(SC_6F_4\text{-}4\text{-}H)_2]$ (**1**) and $[SnPh_2(SC_6F_5)_2]$ (**2**) with *cis*-$[Pt(PPh_3)_2(Cl)_2]$ afforded the complexes *cis*-$[Pt(PPh_3)_2(SC_6F_4\text{-}4\text{-}H)]$ (**3**) and *cis*-$[Pt(PPh_3)_2(SC_6F_5)_2]$ (**4**) in good yields. Analysis of these products by ^1H NMR exhibit in both cases signals in the aromatic region due to the phenyl groups present in the molecules and analogously to complex **1**, the spectra of complex **3** shows a multiplet centered in 6.62 ppm that evidences the presence of the *para* proton in the $^-SC_6F_4$-4-**H** group. The $^{31}P\{^1H\}$ NMR experiments for the two complexes show unique signals flanked by their corresponding satellites at 19.12 and 18.85 ppm for **3** and **4**, respectively with coupling constant values of $^1J_{P-Pt}$ equal to 3.1 kHz in both cases, these data being in agreement with both phosphorus being magnetically equivalent and arranged in a *cis* conformation [19]. Evidence obtained from the analysis of both complexes by $^{19}F\{^1H\}$ NMR exhibits the presence of the fluorinated fragments, with signals observed at −133.85 and −142.11 ppm for the *ortho* and *meta* fluorine atoms of the $^-SC_6\mathbf{F}_4$-4-H ligand in **3** and multiplets at −133.65, −161.98 and −164.88 for the *ortho*, *meta* and *para* fluorines in the $^-SC_6\mathbf{F}_5$ ligands for complex **4**. Additionally, analysis by FAB^+-MS shows in both cases the molecular ion at 1081 and 1117 *m*/*z* for **3** and **4**, respectively. Furthermore, results obtained from elemental analysis of the two complexes are also in agreement with the proposed formulations.

For the two complexes, *cis*-$[Pt(PPh_3)_2(SC_6F_4\text{-}4\text{-}H)_2]$ (**3**) (Fig. 4) and *cis*-$[Pt(PPh_3)_2(SC_6F_5)_2]$ (**4**), (Fig. 5) we were able to obtain single crystals suitable for their X-ray diffraction analysis, the structures obtained confirm unequivocally the *cis* arrangement assumed above from the NMR data, showing both platinum centers into slightly distorted square planar environments having the two triphenylphosphines in a *cis* arrangement and completing the coordination the two thiolate ligands also allocated in a *cis* arrangement around the metal. In both cases, the bond distances and angles are within the expect values [20]. It is noteworthy that the number of structurally analyzed compounds with the kernel *cis*-$[Pt(SR)_2(PPh_3)_2]$ is comparably large with respect to the corresponding *trans* isomers. This must be attributed to the fact that merely bi-dentate ligands such as S–S ligands [21,22], P–P ligands [23], or both types [21,24] were used allowing exclusively *cis* arrangement and

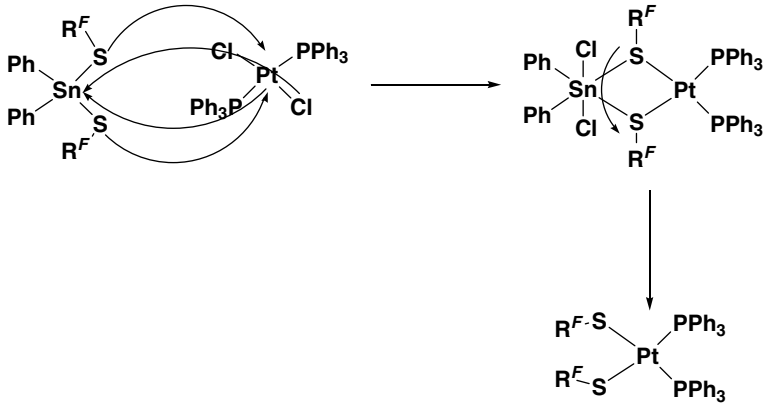

Scheme 2. A proposal of the probable steps involved in the formation of the complexes *cis*-[Pt(PPh$_3$)$_2$(SR^F)$_2$].

at the same time avoiding the very well known polymerization of these complexes. Thus, examples of motifs with exclusively mono-dentate S and P ligands in a *cis* arrangement are rare [25].

It is possible that the formation of these complexes may proceed via a transmetallation reaction (Scheme 2), thus promoting the formation of the *cis* isomer exclusively.

Analogous experiments using the palladium starting material *trans*-[Pd(PPh$_3$)$_2$(Cl)$_2$] with stoichiometric amounts of complexes [SnPh$_2$(SC$_6$F$_4$-4-H)$_2$] (**1**) and [SnPh$_2$(SC$_6$F$_5$)$_2$] (**2**) afforded compounds [Pd(PPh$_3$)(SC$_6$F$_4$-4-H)(μ-SC$_6$F$_4$-4-H)]$_2$ (**5**) and [Pd(PPh$_3$)(SC$_6$F$_5$)(μ-SC$_6$F$_5$)]$_2$ (**6**) in good yields. In both cases analysis by ^{1}H NMR revealed the presence of aromatic protons, and as is for the case of complexes **1** and **3** signals due to the presence of the *para* proton in the $^-$SC$_6$F$_4$-4-**H** group are observed for complex **5**. However in these cases the ^{1}H NMR spectra are more complicated, exhibiting a considerable number of signals indicative of a probable dynamic equilibrium. These results were expected given the proposed formulations for the dimeric species obtained, where the sulfur inversion process may lead to the observation in the NMR time scale of the different probable isomers in solution, i.e. *syn*, *anti*, etc. [26]. Thus, VT NMR experiments were performed with the aim of attain clear information to identifying the probable structure of the complexes **5** and **6**, thus ^{19}F{^{1}H} NMR were collected at temperatures as low as 205 K in CDCl$_3$, however even at these temperatures the coalescence of signals was not reached and the interpretation of the NMR spectra resulted difficult, additionally it was noted that complex **5** was unstable in solution progressively given place the initially red-orange solution to an insoluble dark orange precipitate. Thus, experiments carried out at higher temperatures were performed only with complex **6**. Hence experiments at 330 K afforded an ^{19}F{^{1}H} NMR spectra were six signals (multiplets) can be clearly identified, two corresponding to the *ortho*-fluorines at −126.2 (bridge) and −131.3 (terminal) ppm, two more due to the fluorines in the *para* positions at −148.0 (bridge) and −155.5 (terminal) ppm and finally two more signals due to the *meta*-fluorines at −159.6 (bridge) and −163.5 (terminal) ppm. ^{31}P{^{1}H} NMR experiments of this complex at the same temperature exhibits two signals at 28.27 and 28.11 ppm, these signals being probably due to the *syn* and *anti* isomers for the molecule. Additionally, analysis of both complexes by FAB$^+$-MS shows peaks corresponding to the molecular ion less one thiolate fragment at 1381 *m*/*z* [M$^+$−SC$_6$F$_4$-4-H] for compound **5** and at 1335 *m*/*z* [M$^+$−SC$_6$F$_5$] for complex **6**. This information and that obtained from the elemental analyses agrees in both cases with the proposed formulations.

Crystals of **6** suitable for single crystal X-ray diffraction analysis were obtained by slow diffusion of methanol on a saturated solution of **6** in dichloromethane. The structure obtained shows a dimeric palladium compound (Fig. 6) with the two palladium centers located into slightly distorted square planar environments and bridged by two $^-$SC$_6$F$_5$ thiolate ligands, the coordination of the palladiums is completed by one terminal thiolate $^-$SC$_6$F$_5$ and one PPh$_3$ ligands. Both the bridge and terminal thiolates are arranged in an *anti* conformation and the PPh$_3$ ligands are arranged in a mutually *trans* conformation. The bond distances and angles are typical and comparable to those observed in similar bimetallic structures [27]. These results clearly show that the proposed structures for complexes **5** and **6** are indeed dimeric. The fact that in the case of palladium bimetallic species were obtained is due to the inherent properties of this metal, that along the periodic table (Ni, Pd and Pt) the propensity of these group of metals to polymerize increases from Pt to Ni, this fact may also explain the decomposition (polymerization) of complex [Pd(PPh$_3$)(SC$_6$F$_4$-4-H)(μ-SC$_6$F$_4$-4-H)]$_2$ (**5**) in solution, since the thiolate $^-$SC$_6$F$_4$-4-H is not big enough nor electron-withdrawn enough to avoid the polymerization via the sulfur atom, thus generating insoluble polymers after prolonged times in solution, probably due to the loss of the PPh$_3$ ligands. This fact may also account for the results obtained when analogous reactions carried out using the nickel starting material *trans*-[Ni(PPh$_3$)$_2$(Cl)$_2$] afforded in both cases green insoluble powders, these polymeric species were not further analyzed.

In summary, we have shown that by using the tin(IV) thiolate complexes of the type [SnPh$_2$(SR^F)$_2$]SR^F = $^-$SC$_6$F$_5$ (**1**), $^-$SC$_6$F$_4$-4-H (**2**) we can stereoselectively syn-

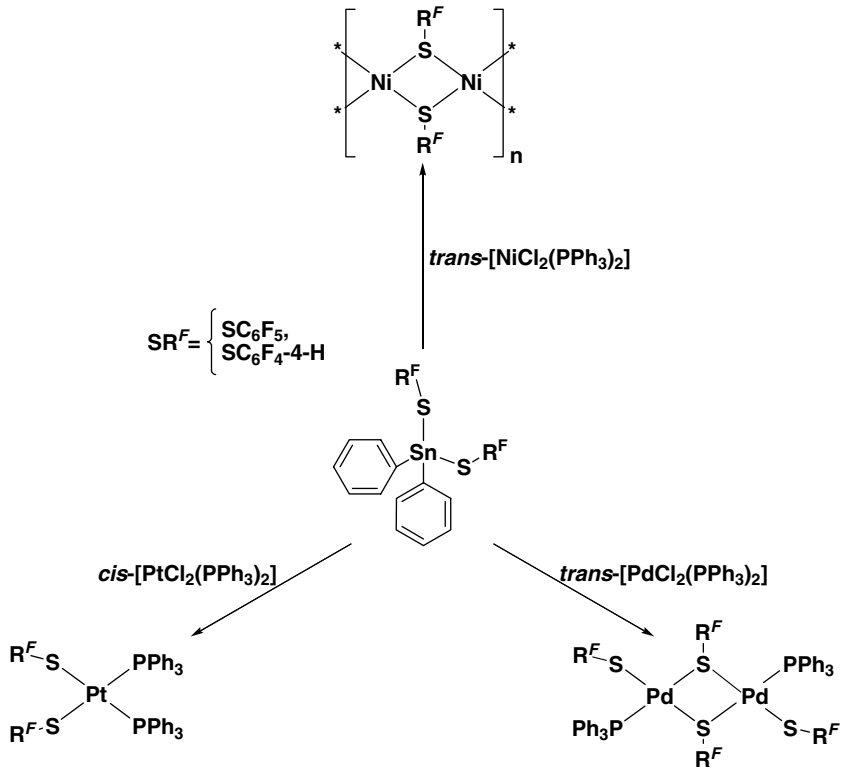

Scheme 3.

thesize through transmetallation reactions the *cis* isomers of the complexes *cis*-[Pt(PPh_3)$_2$(SC_6F_4-4-H)] (**3**) and *cis*-[Pt(PPh_3)$_2$(SC_6F_5)$_2$] (**4**) in good yields, it is probable that similar species are formed when the palladium starting material *trans*-[Pd(PPh_3)$_2$(Cl_2)] is employed, however in this case the formation of dimeric species is observed driven by the intrinsic properties of the metal and the steric and electronic properties of the fluorinated thiolates employed in these reactions, by the same arguments polymeric species are obtained when the nickel starting material *trans*-[Ni(PPh_3)$_2$(Cl_2)] is reacted with the tin(IV)-fluorinated thiolate complexes **1** and **2** (Scheme 3).

4. Supplementary material

CCDC 614100, 614101, 614102, 614103, and 614104 contain the supplementary crystallographic data for **1**, **2**, **3**, **4**, and **6**. These data can be obtained free of charge via http://www.ccdc.cam.ac.uk/conts/retrieving.html, or from the Cambridge Crystallographic Data Centre, 12 Union Road, Cambridge CB2 1EZ, UK; fax: (+44) 1223-336-033; or e-mail: deposit@ccdc.cam.ac.uk.

Acknowledgements

F.E.-N. thank CONACYT for financial support. We thank Chem. Eng. Luis Velasco Ibarra, M. Sc. Francisco Javier Pérez Flores and Eréndira García Ríos and Ma. de las Nieves Zavala for their invaluable help in the running of the FAB$^+$-mass, IR and $^{19}F\{^1H\}$ spectra, respectively. The support of this research by CONACYT (J41206-Q, J43116-F) and PAPIIT (IN114605, IN106405) is gratefully acknowledged. We are indebted to Dr. Jesus Valdés-Martínez, for its invaluable help in the discussion of the π–π stacking interaction in complex **1**.

References

[1] S. Tabassum, C. Pettinari, J. Organomet. Chem. 691 (2006) 1761.
[2] (a) T. Maher, J. Snyder, P. Durham, N.N. Gerasimchuk, in: Proceedings of the 229th ACS National Meeting, San Diego, CA, United States, March 13–17 (2005) INOR-719 (Abstracts);
(b) M. Gielen, J. Braz. Chem. Soc. 14 (2003) 870, and references therein;
(c) C.T. Chasapis, S.K. Hadjikakou, A. Garoufis, N. Hadjiliadis, T. Bakas, M. Kubicki, Y. Ming, Bioinorg. Chem. Appl. 2 (2004) 43;
(d) N. Hoeti, D.E. Zhu, Z. Song, Z. Wu, S. Tabassum, M. Wu, J. Pharmacol. Exp. Ther. 311 (2004) 22;
(e) N. Hoeti, J. Ma, S. Tabassum, Y. Wang, M. Wu, J. Biochem. 134 (2003) 521;
(f) N.M. Xanthopoulou, S.K. Hadjikakou, N. Hadjiliadis, M. Schurmann, K. Jurkschat, A. Michaelides, S. Skoulika, T. Bakas, J. Binolis, S. Karkabounas, K. Charalabopoulos, J. Inorg. Biochem. 96 (2003) 425.
[3] (a) A.P. Dove, V.C. Gibson, E.L. Marshall, A.J.P. White, D.J. Williams, Chem. Commun. (2001) 283;
(b) N. Nimitsiriwat, E.L. Marshall, V.C. Gibson, M.R.J. Elsegood, S.H. Dale, J. Am. Chem. Soc. 126 (2004) 13598;
(c) J.L. Faure, H. Gornitzka, R. Reau, D. Stalke, G. Bertrand, Eur. J. Inorg. Chem. (1999) 2295;
(d) K.B. Aubrecht, M.A. Hillimyer, W.B. Tolman, Macromolecules 35 (2002) 644;

(e) R. García-Zarracino, H. Höpfl, J. Am. Chem. Soc. 127 (2005) 3120.
[4] (a) D. Milstein, J.K. Stille, J. Am. Chem. Soc. 101 (1979) 4992;
(b) D.J. Cárdenas, Angew. Chem., Int. Ed. Engl. 42 (2003) 384;
(c) K. Fugami, M. Kosugi, Organotin Compounds, in: N. Miyaura (Ed.), Cross Coupling Reactions. A Practical Guide. Topics in Current Chemistry, vol. 219, Springer, 2002, p. 87.
[5] P. Espinet, A.M. Echavarren, Angew. Chem., Int. Ed. 43 (2004) 4704.
[6] (a) I. Bertini, H.B. Gray, S.J. Lippard, J.S. Valentine, Bioinorganic Chemistry, University Science Books, USA, 1994 (Chapter 7);
(b) D.H. Nguyen, H.-F. Hsu, M. Millar, S.A. Koch, J. Am. Chem. Soc. 118 (1996) 8963;
(c) J.D. Niemoth-Anderson, K.A. Clark, T.A. George, C.R. Ross, J. Am. Chem. Soc. 122 (2000) 3977.
[7] (a) L.L. Maisela, A.M. Crouch, J. Darkwa, I.A. Guzei, Polyhedron 20 (2001) 3189;
(b) O. Crespo, F. Canales, M.C. Gimeno, P.G. Jones, A. Laguna, Organometallics 18 (1999) 3142;
(c) D.-Y. Noh, E.-M. Seo, H.-J. Lee, H.-Y. Jang, M.-G. Choi, Y.H. Kim, J. Hong, Polyhedron 20 (2001) 1939;
(d) V.D. de Castro, G.M. de Lima, A.O. Porto, H.G.L. Siebald, J.D. de Souza Filho, J.D. Ardisson, J.D. Ayala, G. Bombieri, Polyhedron 23 (2004) 63;
(e) T.F. Baumann, J.W. Sibert, M.M. Olmstead, A.G.M. Barrett, B.M. Hoffman, J. Am. Chem. Soc. 116 (1994) 2639.
[8] J.R. Dilworth, J. Hu. Adv. Inor. Chem. 40 (1993) 411.
[9] See for instance: (a) J.R. Dilworth, D. Morales, Y. Zheng, J. Chem. Soc. Dalton. Trans. (2000) 3007;
(b) V. Gómez-Benítez, R.A. Toscano, D. Morales-Morales, Inorg. Chem. Commun. (2006), doi:10.1016/j.inoche.2006.08.020.
[10] (a) D. Morales-Morales, R. Redón, Y. Zheng, J.R. Dilworth, Inorg. Chim. Acta. 328 (2002) 39;
(b) J.R. Dilworth, P. Arnold, D. Morales, Morales Morales, Y.L. Wong, Y. Zheng, in: The Chemistry and Applications of Complexes with Sulfur LigandsModern Coordination Chemistry, The Legacy of Joseph Chatt, Cambridge, UK, 2002, p. 217.
[11] L.M. Venanzi, J. Chem. Soc. (1958) 719.
[12] L. Malatesia, M. Angoletta, J. Chem. Soc. (1957) 1186.
[13] R.D. Gillard, M.F. Pilbrow, J. Chem. Soc. Dalton. (1974) 2320.
[14] M.E. Peach, Can. J. Chem. 46 (1968) 2699.
[15] G.M. Sheldrick, Acta Crystallogr., Sect. A 46 (1990) 467.
[16] SHELXL-97, Program for Crystal Structure Refinement, University of Göttingen, 1998.
[17] L.J. Farrugia, J. Appl. Crystallogr. 30 (1997) 565.
[18] (a) T. Dahl, Acta Crystallogr., Sect. B 33 (1997) 3021;
(b) C.J.J. Janiak, J. Chem. Soc., Dalton Trans. (2000) 3885.
[19] L.D. Quin, J.G. Verkade, Phopshorus-31 NMR Spectral Properties in Compound Characterization and Structural Analysis, Wiley, 1994.
[20] (a) R. Redón, R. Cramer, S. Bernès, D. Morales, H. Torrens, Polyhedron 20 (2001) 3119;
(b) J. García, E. Martín, D. Morales, H. Torrens, Inorg. Chim. Acta. 207 (1993) 93;
(c) R. Redón, H. Torrens, Z. Wang, D. Morales-Morales, J. Organomet. Chem. 654 (2002) 16;
(d) O. Baldovino-Pantaleon, G. Ríos-Moreno, R.A. Toscano, D. Morales-Morales, J. Organomet. Chem. 690 (2005) 2880;
(e) C. Herrera-Álvarez, V. Gómez-Benítez, R. Redón, J.J. García, S. Hernández-Ortega, R.A. Toscano, D. Morales-Morales, J. Organomet. Chem. 689 (2004) 2464.
[21] J. Forniés-Cámer, A. Aaliti, N. Ruiz, A.M. Masdeu-Bultó, C. Claver, C.J. Cardin, J. Organomet. Chem. 530 (1997) 199.
[22] (a) S.A. Bryan, D.M. Roundhill, Acta Crystallogr., Sect. C 39 (1983) 184;
(b) M.J.G. Lesley, W. Clegg, T.B. Marder, N.C. Norman, A.G. Orpen, A.J. Scott, J. Starbuck, Acta Crystallogr., Sect. C 55 (1999) 1272;
(c) D.S. Dudis, C. King, J.P. Fackler Jr., Inorg. Chim. Acta 181 (1991) 99;
(d) C.E. Keefer, S.T. Purrington, R.D. Bereman, B.W. Knight, D.R. Bedgood Jr., P.D. Boyle, Inorg. Chim. Acta. 282 (1998) 200.
[23] (a) M. Capdevila, W. Clegg, P. Gonzáles-Duarte, B. Harris, I. Mira, J. Sola, I.C. Taylor, J. Chem. Soc., Dalton Trans. (1992) 2817;
(b) G. Wei, H. Liu, Acta Crystallogr., Sect. C 46 (1990) 2457.
[24] J.M. Bevilacqua, J.A. Zuleta, R. Eisenberg, Inorg. Chem. 33 (1994) 258.
[25] (a) Q. Chen, F. Boeheim, J. Dabrowiak, J. Zubieta, Inorg. Chim. Acta. 216 (1994) 83;
(b) C.E. Briant, G.R. Hughes, P.C. Minshall, D.M.P. Mingos, J. Organomet. Chem. 202 (1980) C18;
(c) R. Vicente, J. Ribas, X. Solans, G. Germain, An. Quim. Ser. B. 82 (1986) 47.
[26] R. Redón, H. Torrens, F.E. Hahn, T. Lügger, S. Hernández-Ortega, R.A. Toscano, D. Morales-Morales, J. Mol. Struct. 655 (2003) 423.
[27] V.K. Jain, L. Jain, Coord. Chem. Rev. 249 (2005) 3075.
[28] X-Seed program: J.L. Barbour, J. Supramol. Chem. 1 (2001) 189.